

# Manipulating signal delivery – plasma-membrane ERK activation in aPKC-dependent migration

Katrina Boeckeler<sup>1</sup>, Carine Rosse<sup>1</sup>, Michael Howell<sup>2</sup> and Peter J. Parker<sup>1,3,\*</sup>

<sup>1</sup>Protein Phosphorylation Laboratory, Cancer Research UK, London Research Institute, 44 Lincoln's Inn Fields, London, WC2A 3PX, UK

<sup>2</sup>High-throughput Screening Laboratory, Cancer Research UK, London Research Institute, 44 Lincoln's Inn Fields, London, WC2A 3PX, UK

<sup>3</sup>Division of Cancer Studies, King's College London, Guy's Hospital, London, SE1 1UL, UK

\*Author for correspondence ([peter.parker@caner.org.uk](mailto:peter.parker@caner.org.uk))

Accepted 10 May 2010

Journal of Cell Science 123, 2725-2732

© 2010. Published by The Company of Biologists Ltd

doi:10.1242/jcs.062299

## Summary

Members of the PKC superfamily have been implicated in various migratory models and in particular in spatially restricted processes. However, defining the precise local events that underlie the PKC-dependent processes is constrained by the unspecific nature of interventions. Here we address this problem in relation to atypical PKC (aPKC) action, which in conjunction with the exocyst complex controls the polarised delivery of promigratory signals. A drug-dependent recruitment approach was employed to manipulate the local recruitment of signals to the leading edge of migrating cells, under conditions where the aPKC-exocyst control is globally abrogated. We found that activation of ERK but not JNK at focal adhesions recovers the majority of the migratory loss attributed to ERK action, demonstrating a necessary role for active plasma membrane ERK in the downstream signalling of aPKC-dependent migration. The data further show that restored focal adhesion dynamics are a contributing mechanism through which localized ERK activity influences this aPKC-exocyst-dependent migration.

**Key words:** aPKC, ERK, Exocyst, Migration, JNK, Paxillin, Kibra, Rapalogue

## Introduction

The correct distribution of signalling molecules to specific subcellular locations is a key element in the successful transmission of signals in a cell. Highly ordered cellular processes such as polarisation and migration are dependent on the coordination of localised events, distinguishing, for example, focal adhesion behaviour at the leading and trailing edges of cells. Typically the machinery that establishes such behaviour, alongside the associated hierarchy of regulators, are shared across multiple compartments and this limits the conclusions that can be drawn following the global inhibition or silencing of these players.

Atypical PKC isoforms (aPKC $\zeta$  and aPKC $\iota$ ) have been demonstrated to be involved in polarisation and migration as evidenced in many models. An aPKC-Par complex is involved in migration and in maintaining apical-basal polarity in multiple contexts (reviewed by Suzuki and Ohno, 2006). Both aPKCs are also associated with HeLa cell migration where they phosphorylate the endocytotic adaptor protein Numb allowing endocytosis of integrins at the leading edge (Nishimura and Kaibuchi, 2007). It has been shown in lung cancer cells that aPKC $\iota$  promotes nicotine-induced migration and invasion via phosphorylation of calpains (Xu and Deng, 2006). aPKC $\zeta$  is implicated with Smurf1 in EGF-induced chemotaxis in human breast cancer cells (Sun et al., 2005) as well as via GSK-3 in Golgi and centrosome polarity in migrating astrocytes (Etienne-Manneville and Hall, 2003). Furthermore, aPKC $\zeta$  complexes with Par6 to regulate the spatially localized association of mammalian Dlg1 and APC, controlling cell polarization (Etienne-Manneville et al., 2005).

Recently, aPKC has been shown to regulate a distinct migratory pathway in NRK cells (Rosse et al., 2009). This pathway does not involve CDC42-Par6 or secretory events, but rather aPKC acts through a complex with exocyst and kibra, which traffics with

aPKC in a microtubule-dependent fashion to the leading edge of migrating cells (Rosse et al., 2009). This translocation coincides with the activation of ERK and JNK at the leading edge (see Fig. 1A, I). The two MAP kinases phosphorylate downstream targets in this compartment including the focal complex protein paxillin. Global inhibition or depletion of aPKC prevents this signal cascade and blocks the migratory response to a wound (Fig. 1A, II). Hence there is a correlation between aPKC blockade, the loss of ERK and/or JNK activation at the leading edge (but not in other compartments) and a deficit in migratory behaviour. However, this remains a correlation and it is entirely unclear which signals delivered to the leading edge by the aPKC-kibra-exocyst complex are necessary for a migratory response.

To address the question of what is sufficient to suppress the aPKC dependence of signal delivery, under conditions where aPKC function is blocked, we have triggered delivery independently using the dimerization agent rapalogue (Fili et al., 2006; Inoue et al., 2005; Varnai et al., 2006). Exploiting this approach we show that the localized activation of ERK at the leading edge and not the related JNK can indeed partially rescue the loss of aPKC action, restoring focal adhesion dynamics. Thus the aPKC-kibra-exocyst pathway to ERK is not simply a correlation with migratory behaviour but displays a degree of sufficiency in enabling cell migration.

## Results

### The rapalogue dimerization system recruits MEK1 to focal adhesions

To manipulate signals locally at the leading edge in NRK cells, rapalogue (AP21967) was used to induce dimerization of the FK506-binding protein 12 (FKBP)-paxillin fusion with a mutated portion of mTOR/FRAP (FRB\*) fused to upstream signals (Fig.

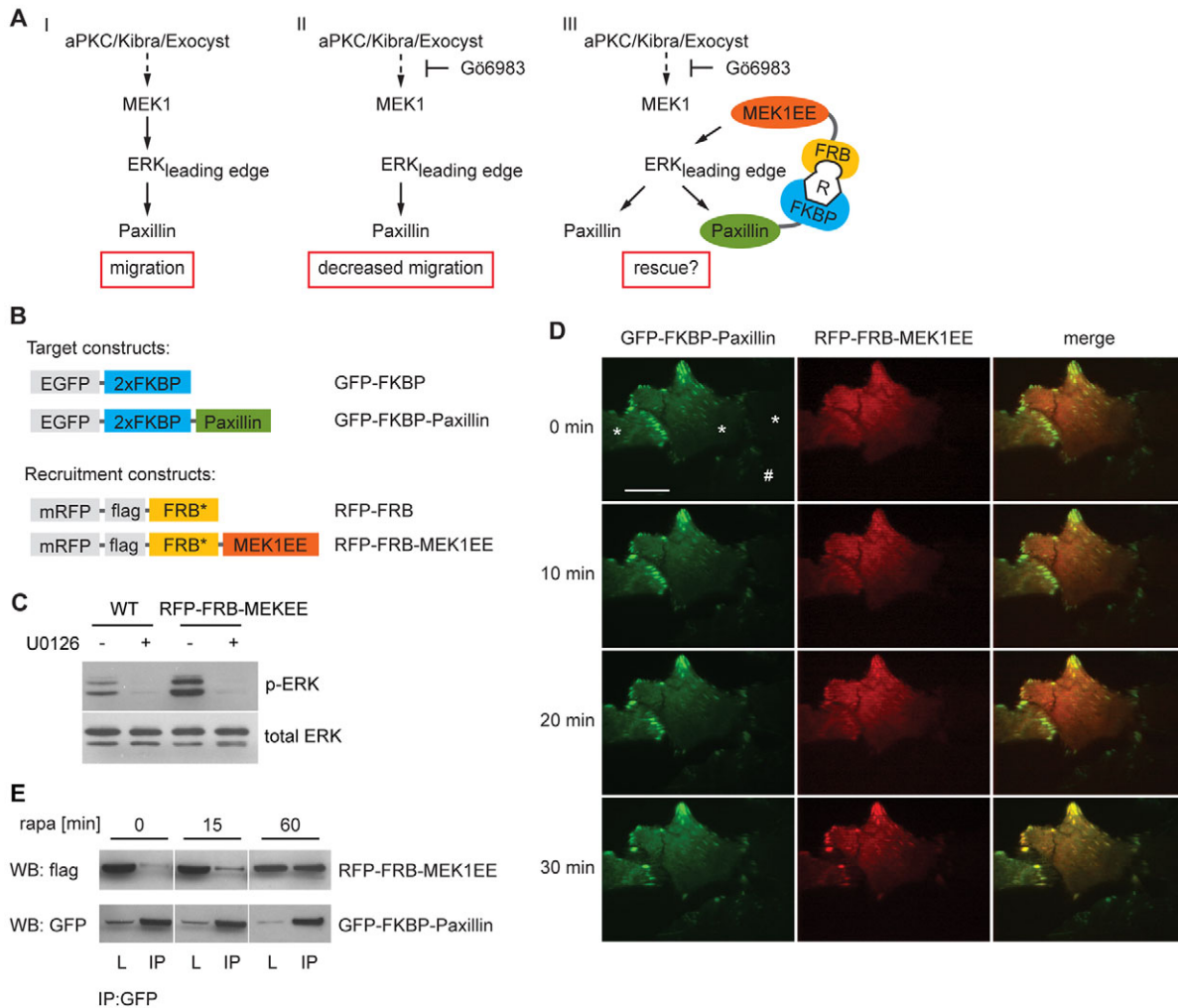


**Fig. 1. Rapalogue-induced recruitment of MEK1EE to paxillin.** (A) Schematic illustrating the signal 'delivery' pathway under analysis (I), the blockade of that pathway (II) and the delivery of one element of this cascade through drug action (III). (B) Paxillin and MEK1EE were fused to 2xFKBP and a mutated FRB domain, respectively. MEK1EE bears a double mutation (S218E and S222E) for constitutive activation. (C) Wild-type NRK cells and NRK cells expressing RFP-FRB-MEK1EE were treated for 3 hours with 10  $\mu$ M U0126. ERK1/2-*P* and total ERK1/2 were detected by western blotting. (D) NRK cells transiently transfected with GFP-FKBP-paxillin and RFP-FRB-MEK1EE were treated with 300 nM rapalogue. Images were taken every minute with a TIRF microscope. Representative images before and after 10-, 20- and 30-minute rapalogue treatments are shown (see also supplementary material Movie 1). Asterisks indicate cells expressing both fusion proteins; the hash (#) indicates cell expressing only GFP-FKBP-paxillin. Scale bar: 20  $\mu$ m. (E) NRK cells stably expressing GFP-FKBP-paxillin and RFP-FRB-MEK1EE were treated with 300 nM rapalogue for the indicated times. GFP-FKBP-paxillin was immunoprecipitated and detected with a GFP antibody. Co-precipitated RFP-FRB-MEK1EE was detected with a FLAG antibody (L, whole cell lysate; IP, precipitate).

1A, III). The selection of paxillin as a suitable target molecule for recruitment was based on previous observations that paxillin is enriched in focal adhesions at the leading edge of migrating cells, and furthermore that in an aPKC-dependent manner it becomes phosphorylated on ERK (serine 126) and JNK (serine 178) sites during migration. For ERK activation a recruitment protein consisting of the MAP2K MEK1EE fused to mRFP, the FRB domain and a FLAG-tag was constructed (RFP-FRB-MEK1EE) (Fig. 1B). MEK1EE carries a double point mutation (S218E/S222E) for constitutive activation (Mansour et al., 1994). Activity of the MEK1EE fusion protein was tested by probing for ERK1/2-*P* (Fig. 1C). Cells expressing the chimera showed elevated phosphorylation of ERK1/2 compared with wild-type cells and in both cases a 3-hour incubation with the MEK1 inhibitor U0126 (10  $\mu$ M) prevented phosphorylation as expected (Favata et al.,

1998). Fusion proteins without paxillin (GFP-FKBP only) or without MEK1EE (RFP-FRB only) were used as controls. Constructs were expressed in NRK-49 F cells (Yeaman et al., 2001) and stable cell lines selected with puromycin or hygromycin as appropriate for the vector.

GFP-FKBP-paxillin localised in NRK cells as expected in characteristic focal adhesion patches whereas RFP-FRB-MEK1EE was found evenly distributed in the cytosolic compartment. Upon adding 300 nM rapalogue the MEK1EE fusion protein translocated to focal adhesions (Fig. 1D and supplementary material Movie 1). Recruitment of the mRFP-labelled protein reached a maximum after 30 minutes. It should be noted that only a portion of the expressed fusion protein was recruited to the focal adhesions and that there was still RFP-FRB-MEK1EE present in the cytosol. Rapalogue-induced dimerization was also tested by co-

immunoprecipitation (Fig. 1E). There was some minor association of GFP-FKBP-paxillin and RFP-FRB-MEK1EE already before the addition of rapalogue, as previously observed by other groups (Ishibe et al., 2003; Slack-Davis et al., 2003) but association was greatly increased after rapalogue treatment in a time-dependent manner.

### Recruitment of MEK1EE leads to phosphorylation of ERK at focal adhesions

Rosse et al. (Rosse et al., 2009) reported the loss of localized ERK1/2 activation at the leading edge upon treatment of cells with the PKC inhibitor Gö6983 or depletion of aPKC by siRNA. Although Gö6983 is a pan-PKC inhibitor (cPKC, nPKC, aPKC), results with two more discriminating PKC inhibitors, BIM1 (cPKC, nPKC) and Gö6976 (cPKC), alongside the siRNA data demonstrated that the loss of ERK-*P* and subsequent block in cell migration is aPKC dependent. Based on these precedents we

employed Gö6983 and siRNA directed at aPKCs to block the aPKC migratory pathway.

To assess the effect of paxillin-recruited MEK1EE on ERK1/2 activation in NRK cells stably expressing GFP-FKBP-paxillin and RFP-FRB-MEK1EE, we examined ERK1/2 phosphorylation at focal adhesions by immunofluorescence (Fig. 2A). Cells were wounded and treated with Gö6983 for 4 hours followed by treatment without or with rapalogue for 1 hour before fixation. In agreement with previous work (Ishibe et al., 2003) phosphorylated ERK1/2 is present at focal adhesions under control migratory conditions where it is assumed to control focal adhesion and actin dynamics (Fincham et al., 2000; Pawlak and Helfman, 2002; Webb et al., 2004). Under control conditions, recruitment of MEK1EE in response to rapalogue has no obvious effect since the intensity of the ERK1/2-*P* signal does not increase significantly. aPKC inhibition, however, prevents ERK1/2 phosphorylation at focal adhesions in migrating cells. This leading-edge defect in ERK1/2

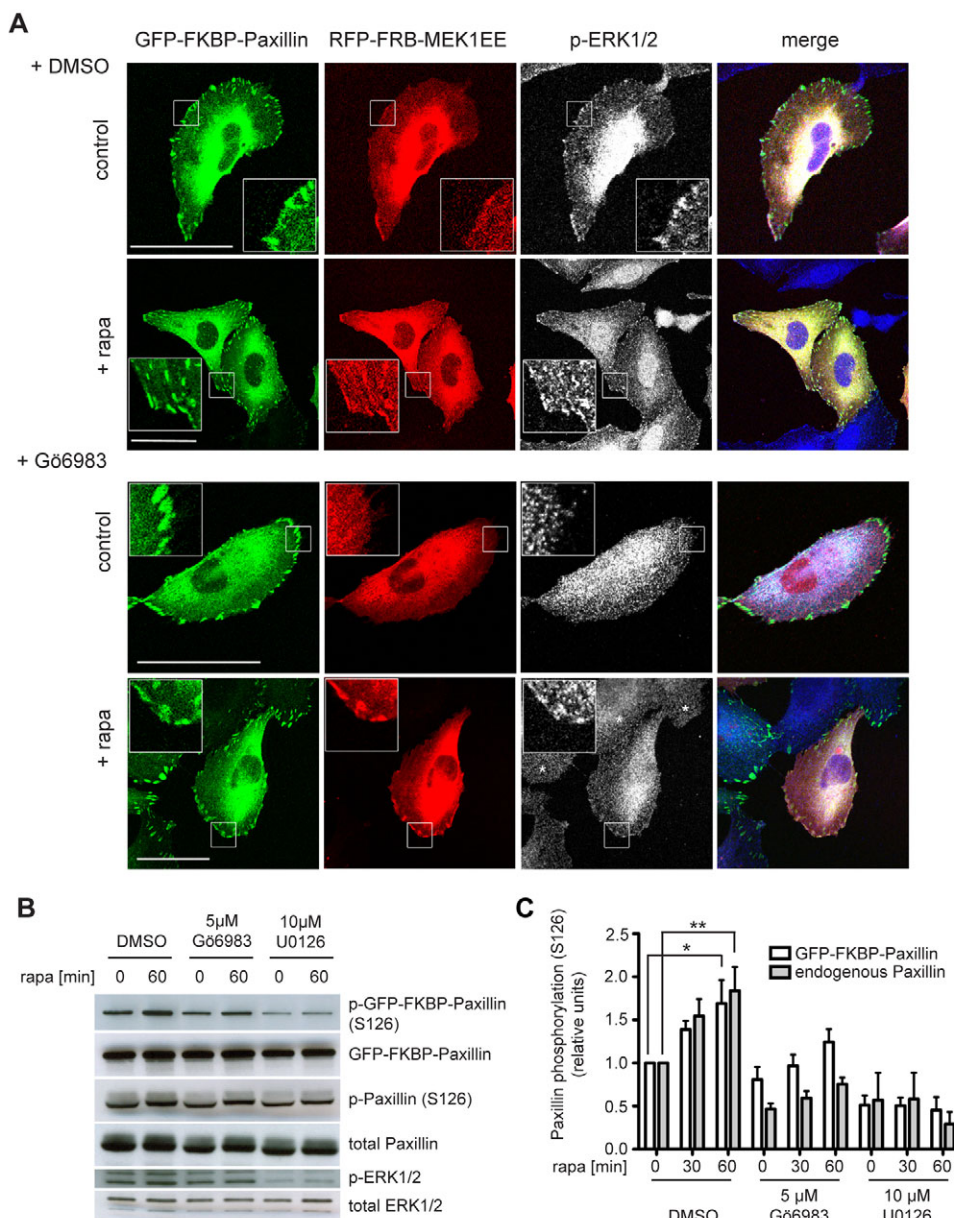


### Fig. 2. Recruitment of MEK1 leads to phosphorylation of ERK and paxillin at focal adhesions.

(A) Monolayers of NRK cells expressing GFP-FKBP-paxillin and RFP-FRB-MEK1EE were wounded and treated with 5 µM PKC inhibitor Gö6983 for 3 hours followed by treatment with 300 nM rapalogue for 60 minutes as indicated. Cells were fixed and immunostained for ERK1/2-*P*. Asterisks indicate control cells without recruitment. Insets show areas of interest magnified 3×. Scale bars: 50 µm.

(B) Monolayers of confluent NRK cells stably expressing GFP-FKBP-paxillin and RFP-FRB-MEK1EE were extensively scratched to maximize the number of free edges. Cells were first treated with 5 µM Gö6983 or 10 µM U0126 for 4 hours followed by treatment with 300 nM rapalogue for 60 minutes. Paxillin (S126-*P*), total paxillin, ERK1/2-*P* and total ERK1/2 were detected by western blotting.

(C) Quantification of paxillin phosphorylation at S126. Values are means ± s.e.m. \* $P < 0.05$ , \*\* $P < 0.01$  (ANOVA).

phosphorylation is reversed in response to rapalogue through recruitment of MEK1EE to paxillin, but only in cells expressing both fusion proteins, in which ERK1/2-*P* staining colocalizes with focal adhesion patches (Fig. 2A, arrows). Note the absence of ERK1/2-*P* at focal adhesions in cells with no RFP-FRB-MEK1EE expression (Fig. 2A, asterisk). This indicates that rapalogue-induced recruitment of MEK1EE to paxillin leads to phosphorylation of ERK at focal adhesions under conditions where the normal pathway to activation in this compartment is blocked by Gö6983.

### Recruitment of MEK1 leads to phosphorylation of paxillin in a time-dependent manner

We next investigated whether the ability of recruited MEK1EE to locally activate ERK1/2 is sufficient to also affect paxillin phosphorylation. There are published reports of several ERK phosphorylation sites in paxillin, with some of them directly implicated in cell migration (Ishibe et al., 2003; Liu et al., 2002; Webb et al., 2005; Woodrow et al., 2003). In this study we used a phospho-specific antibody to the S126 site as a marker for the phosphorylation of paxillin by ERK. Western blot analyses of cell lysates from wounded NRK cells stably expressing GFP-FKBP-paxillin and RFP-FRB-MEK1EE showed that treatment with rapalogue for 60 minutes led to an increase in the phospho-signal of the ectopically expressed paxillin as well as of the endogenous paxillin (Fig. 2B). In addition, we observed an electrophoretic mobility shift very probably due to phosphorylation at additional sites. Consistent with previous data (Rosse et al., 2009) pre-treatment with Gö6983 for 4 hours diminished the basal phosphorylation of paxillin compared with control conditions. The finding that phosphorylation is only partially reduced probably reflects the fact that there are multiple pathways that can influence this phosphorylation with the residual inputs not being under aPKC control. After MEK1EE recruitment there was again an increase in paxillin-*P* and the characteristic mobility shift. To ensure that the induced phosphorylation is the result of the activity of MEK1, cells were pre-exposed to U0126 before rapalogue. A quantitative analysis showed a time-dependent increase in paxillin phosphorylation in response to rapalogue (Fig. 2C). It is unclear why U0216 only inhibits ERK phosphorylation by ~70% unless there is one or more pools of active ERK that turn over very slowly in these cells (not at the focal adhesions). Nevertheless, it is evident that U0216 entirely blocks the paxillin S126 phosphorylation induced by rapalogue treatment, consistent with the action of MEK1EE.

### Localized MEK1 activity leads to a partial rescue of impaired aPKC-dependent migration

The results suggest that the dimerization system can be used to bypass the aPKC dependence for ERK1/2 phosphorylation at the leading edge. Is this ERK1/2 phosphorylation able to rescue the previously demonstrated block in migration of NRK cells caused by aPKC inhibition (Rosse et al., 2009)? In a monolayer scratch-wound healing assay cells were wounded and treated with Gö6983 and with or without rapalogue (Fig. 3A). Wound closure was monitored and the wound area plotted over time to determine the speed of wound closure (Fig. 3B). Treatment with Gö6983 decreased the speed by about 65% (Fig. 3C). In the presence of both Gö6983 and rapalogue, however, this deficit was partially reversed and the speed was now reduced by only 50% compared with the control. Scratch-wound healing assays performed with increasing rapalogue concentrations (50-300 nM) showed a positive

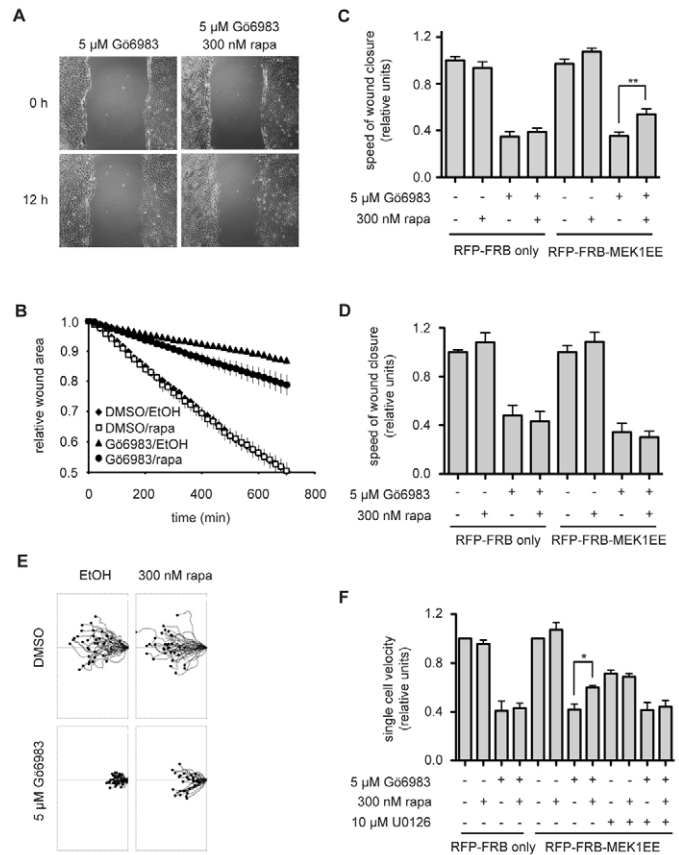


**Fig. 3. Localized MEK1 activity leads to a partial rescue of impaired aPKC-dependent migration.** (A) Confluent monolayers of NRK cells stably expressing GFP-FKBP-paxillin and RFP-FRB-MEK1EE were wounded and treated with 5  $\mu$ M Gö6983 and 300 nM rapalogue. Wound healing was monitored over 12 hours with phase-contrast images that were taken every 20 minutes. (B) Wound closure speed from cells stably expressing GFP-FKBP-paxillin and RFP-FRB-MEK1EE. The data shown represents one of six independent experiments. Speeds of wound closure were determined from the slopes of these graphs (EtOH, ethanol). (C) Paxillin recruitment of a control or MEK1EE fusion protein. Mean wound closure speed of cells stably expressing GFP-FKBP-paxillin and RFP-FRB only ( $n=3$ ) or GFP-FKBP-paxillin and RFP-FRB-MEK1EE ( $n=6$ ). Error bars represent s.e.m.  $**P<0.01$  (ANOVA). (D) Vector control recruitment of a control or MEK1EE fusion protein; bar graph of mean wound closure speed from cells expressing GFP-FKBP only and RFP-FRB-MEK1EE ( $n=3$ ) or GFP-FKBP only and RFP-FRB only ( $n=3$ ). Error bars represent s.e.m. (E) At least 20 cells from each of three independent wound healing experiments were tracked to determine velocity and persistence. The panels show scatter plots of one representative experiment with cells expressing GFP-FKBP-paxillin and RFP-FRB-MEK1EE. (F) Cell velocities normalized to the control condition for cells expressing GFP-FKBP-paxillin and RFP-FRB only or GFP-FKBP-paxillin and RFP-FRB-MEK1EE ( $n=3$ ) treated with 5  $\mu$ M Gö6983, 10  $\mu$ M U0126 and 300 nM rapalogue. Error bars represent s.e.m.  $*P<0.05$  (ANOVA).

correlation between concentration and migration speed (supplementary material Fig. S1A). Recruitment with a construct that did not contain MEK1EE failed to show any effect (Fig. 3C) suggesting a catalytic activity or scaffold requirement for the kinase. Furthermore, using a similar fusion construct for an activated form of the MAP2K for JNK, MKK4EE, there was no significant effect on migration, even though rapalogue recruitment of the kinase could be shown to induce paxillin phosphorylation

**Table 1. Single cell velocity in scratch-wound healing assay**

Expressed protein	300 nM rapalogue	5 $\mu$ M Gö6983	10 $\mu$ M U0126	Speed ( $\mu$ m/hour)
GFP-FKBP-paxillin +	–	–	–	12.8 $\pm$ 0.6
RFP-FRB	+	–	–	12.2 $\pm$ 1.0
	–	+	–	5.2 $\pm$ 0.8
	+	+	–	5.5 $\pm$ 0.2
GFP-FKBP-paxillin +	–	–	–	9.5 $\pm$ 0.5
RFP-FRB-MEK1ca	+	–	–	10.1 $\pm$ 0.7
	–	+	–	4.0 $\pm$ 0.5
	+	+	–	5.7 $\pm$ 0.4
	–	–	+	6.5 $\pm$ 0.3
	+	–	+	6.3 $\pm$ 0.5
	–	+	+	3.8 $\pm$ 0.5
	+	+	+	4.0 $\pm$ 0.5

Cell speed is reported as mean  $\pm$  s.e.m. and was determined from 20-30 cells from each of three independent experiments.

on the JNK site (supplementary material Fig. S2). This demonstrates that JNK activation alone at the leading edge is insufficient to influence migration and also provides evidence for a specific effect of MEK1EE.

To check that the spatial effect is dependent on targeting MEK1EE to focal adhesions the scratch-wound healing assay was performed with cells expressing the GFP-labelled FKBP domain not fused to paxillin. This fusion protein is located in the cytoplasm and nucleus and dimerizes with the MEK1EE chimera in the same manner as the paxillin fusion construct (supplementary material Fig. S2B,C). No difference in wound closure speed after rapalogue treatment could be detected, indicating that MEK1EE has to be located with paxillin enriched at the focal adhesions to trigger the accelerated migration observed in the presence of Gö6983 (Fig. 3D). Notwithstanding the finding that random recruitment to a GFP fusion protein does not influence migration (controlling for non-specific effects), it remains possible that specific recruitment of MEK1EE to paxillin at sites other than the plasma membrane might influence migration and focal adhesion turnover indirectly. Currently we cannot rule this out, but the most likely explanation is that the effect is driven through plasma-membrane-localised paxillin recruitment and the influence there on focal adhesion dynamics (see below).

The persistence of migrating cells was not affected by Gö6983, rapalogue or by their combination (Fig. 3E); however, cell velocity was altered. The average speed of untreated migrating cells was 9.5  $\mu$ m/hour and treatment with Gö6983 reduces this to 4  $\mu$ m/hour. Addition of rapalogue partially rescues the deficit resulting in a migration speed of 5.7  $\mu$ m/hour and pretreatment with U0126 blocked this rescue (Fig. 3F and Table 1). The extent of recovery of migration accounts in fact for ~60% of the total dependence defined by global MEK inhibition by U0126, suggesting a significant role of ERK activation in aPKC-dependent migration.

Depletion of PKC $\zeta$  with siRNA confirmed the observations made with Gö6983. In these experiments PKC $\zeta$  knock-down alone caused a ~30% reduction in cell speed from 11.7 to 8  $\mu$ m/h with a recovery to 9.6  $\mu$ m/h on addition of rapalogue (supplementary material Fig. S3A-C).

#### Recruitment of MEK1EE reverses the effect of aPKC inhibition on focal adhesion size and turnover

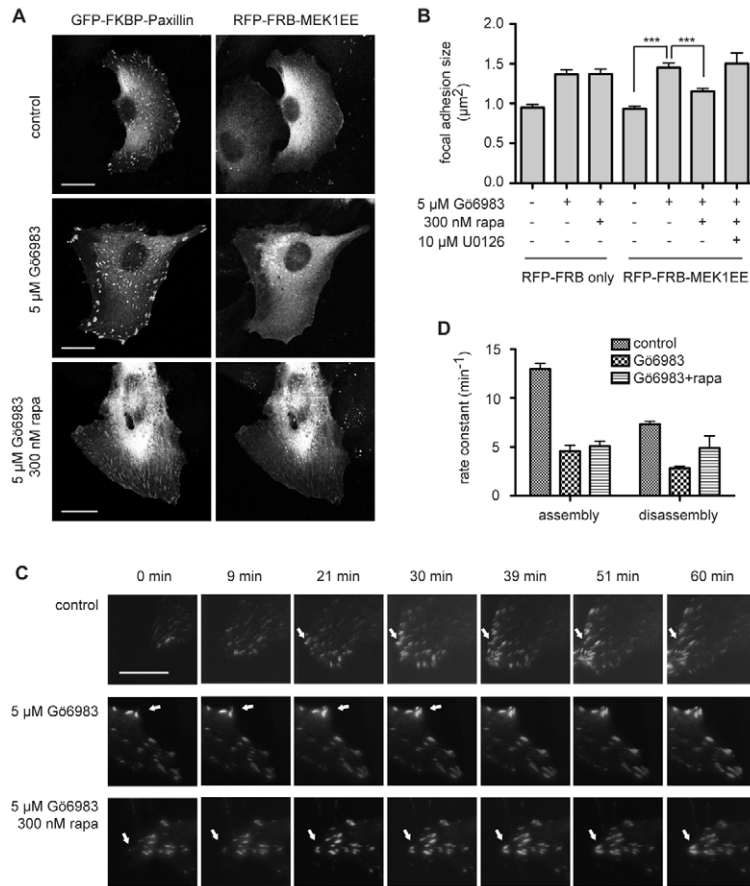
Focal adhesion stability and dynamics largely determine the ability of a cell to migrate (Broussard et al., 2008; Carragher and Frame, 2004; Lock et al., 2008; Ridley et al., 2003; Zaidel-Bar et al.,

2003). To assess how localized ERK1/2-*P* mediates aPKC-dependent migration, the behaviour of focal adhesions were further explored. Confocal images revealed considerably enlarged focal adhesion patches upon aPKC inhibition, as detected by the paxillin fusion construct (Fig. 4A); TIRF immunofluorescence imaging confirmed this observation. These large focal adhesions are indicative of less dynamic structures and less motile cells. We examined more than 400 focal adhesions at the front of migrating cells that expressed GFP-FKBP-paxillin and either RFP-FRB alone or RFP-FRB-MEK1EE. Cells treated with Gö6983 showed a 1.6-fold increase in the mean size of focal adhesions compared with untreated cells in both cell lines (Fig. 4B), suggesting that the defect in migration is mirrored in focal adhesion stability. In accordance with the migratory data, the increase in patch size was reversed by recruitment of MEK1EE with rapalogue but not by recruitment of the FRB domain only. Experiments using the focal adhesion protein zyxin, which is not associated with the recruiting device itself, showed the same pattern of behaviour as observed for paxillin, although the extent of recovery was less impressive (supplementary material Fig. S4).

Employing paxillin as a recruitment target and marker proved to be very useful as it allowed examination of focal adhesion turnover kinetics by following the fluorescence intensity of paxillin over time and measuring the build-up and breakdown of individual patches at the leading edge in migrating cells (Webb et al., 2004) (Fig. 4C). The determined rates of assembly and disassembly are shown in Table 2. Inhibition of PKC leads to an impairment in assembly and disassembly, which is ~40% of control values. Interestingly the addition of rapalogue mainly affects the disassembly rate elevating it to 67% of the rate of control cells.

#### Discussion

The crucial nature of location in the action of signal relays has become increasingly evident with the wealth of evidence becoming available on the influence of membrane traffic, compartments, sub-compartments (e.g. lipid rafts) and scaffolds on signal dynamics. These insights are not matched by our ability to intervene at a subcellular level in order to be able to dissect more precisely the requirements for such localised events. Typically, global inhibition effected by small molecules or siRNA is employed to assess requirements. Such approaches can provide consistent evidence of the need for a particular target, but this lacks the spatial resolution that defines an action in a specific location. Thus, it has been shown previously, by inhibition and siRNA knockdown



experiments (Rosse et al., 2009), that aPKC and the exocyst complex are required for efficient migration in the processes examined here. This requirement correlates with delivery of signals to the leading edge of the cell, but these signals are not unique to the leading edge of the cell, i.e. global inhibition does not define where these signals act to influence migration. By taking the approach of global inhibition and acute, locally induced reactivation of signals, we can start to address the question of which signals delivered to the leading edge are sufficient for this aPKC-exocyst migratory pathway. The evidence presented indicates that with aPKC inhibited, there is a partial rescue when ERK1/2 is reactivated at the leading edge, but not when JNK1/2 is reactivated. This distinction is important in demonstrating the specificity of the recruitment approach employed; equally important are the various controls that establish, for example, the absence of any effects with non-functional fusions. The parsimonious conclusion that can be drawn from this analysis is that ERK1/2 activation at the leading edge is a significant contributory factor in driving the aPKC-

exocyst pro-migratory pathway. MEK1EE recruitment is associated with an increased rate of focal adhesion breakdown representing a substantial reversal of the effect of aPKC inhibition. The implication is that ERK1/2 targets components at the focal adhesion to trigger this response and in this manner contributes to the aPKC control exerted on focal adhesion turnover.

The above conclusion is in agreement with previous findings of an involvement of ERK recruitment to focal adhesions, through the scaffold protein RACK1, which determines focal adhesion turnover (Webb et al., 2004). However, RACK1 is a broad specificity scaffold and siRNA silencing as a means of defining a promigratory role for focal-adhesion-associated ERK does not provide the compelling evidence obtained here from direct activator recruitment. For example, FAK, another focal-adhesion-associated protein, is also scaffolded by RACK1 and has been shown to be regulated downstream of c-abl phosphorylation of RACK1 (Kiely et al., 2009). Nonetheless, the predictions arising out of the RACK1-ERK link do suggest that the role of aPKC-kibra-exocyst in activating ERK might be mediated through the Raf-MEK-ERK cascade, reported to be RACK1 associated in focal adhesions (Webb et al., 2004).

Although paxillin has proved to be a useful vehicle here on multiple levels, i.e. as an ERK- and JNK-targeted device, for recruitment of MEK1EE and MKK4EE, and for the monitoring of focal adhesion behaviour, paxillin is not the only substrate through which ERK might influence migration and focal adhesion stability. Other possible substrates include myosin-light chain kinase (MCLK), shown to regulate late focal adhesion disassembly

**Fig. 4. Recruitment of MEK1 reverses the effect of aPKC inhibition on focal adhesion size and turnover.** (A) Monolayers of NRK cells expressing GFP-FKBP-paxillin and RFP-FRB-MEK1EE were wounded and treated with 5 μM Gö6983 and 300 nM rapalogue. After 3 hours images were taken. Scale bars: 20 μm. (B) Quantification of focal adhesion size. At least 10 cells (>400 focal adhesions) were measured for each treatment. Values are means ± s.e.m. (C) Monolayers of NRK cells stably expressing GFP-FKBP-paxillin and RFP-FRB-MEK1EE plated on fibronectin were wounded and treated with 5 μM Gö6983 and 300 nM rapalogue. After 3 hours images were taken every 3 minutes with a TIRF microscope. Scale bar: 5 μm. See also supplementary material Movie 1. (D) To quantify the rates of assembly and disassembly, the fluorescence intensity of individual adhesions was measured over time. Changes in fluorescence intensity were normalized to the maximal value and plotted in semilogarithmic plots as a function of time. The rates were determined from the slopes of the graphs.

(Klemke et al., 1997; Nguyen et al., 1999; Webb et al., 2004), calpains, which stimulate actin and focal adhesion disassembly (Bhatt et al., 2002; Franco et al., 2004), as well as cortactin, which promotes rearrangement of the actin cytoskeleton (Campbell et al., 1999; Lai et al., 2009). It is very likely that ERK activity at the plasma membrane exerts control on migration via several downstream targets.

The effects observed involving paxillin might in principle be skewed by the fact that paxillin is used as the recruitment partner, necessarily in the form of a fusion protein, which might influence behaviour. Furthermore not all paxillin is located at focal adhesions with broad distribution in the cytosol to which the activated MAPkinase kinases might be recruited. It is noted, however, that MEK1EE is itself constitutively in the cytosol in its active state, both before and after rapalogue treatment. As such, the particular focal-adhesion-localising response is the distinctive event that rapalogue drives and hence it would appear to be this that is responsible for the partial recovery of migration and focal adhesion turnover under conditions of aPKC inhibition. It remains possible that recruitment of MEK1EE to paxillin in a cytosolic sub-compartment does influence migration, however, given the behaviour of focal adhesions on MEK1EE recruitment, it would seem that focal adhesion recruitment was the overriding influence.

Finally, it is appropriate to comment on the potential underlying reasons for the partial rescue of migratory behaviour on the induced activation of ERK at focal adhesions and the leading edge. In principle, the most simplistic explanation is that the inhibition of aPKC-exocyst function leads to multiple deficiencies in signal relays at the leading edge and that the activation of ERK under these circumstances can not cover all that is lost. There are, however, other considerations, including the dynamics of ERK activation. In the MEK1EE recruitment mode of activation, ERK activity is switched on constitutively; in normal migrating cells it is anticipated that there is a dynamic determined by the microtubule network that is responsible for the movement of aPKC-exocyst and the associated cargoes, which we surmise includes the upstream effectors of ERK and JNK, amongst others (Rosse et al., 2009). This distinction between constitutive and dynamic activation might have a significant influence on migration rates. Nevertheless, irrespective of the dynamic or additional signal hypothesis, we can conclude that ERK minimally contributes a sufficiency in driving focal adhesion turnover and that this is at least one component of the aPKC-exocyst pathway driving migration.

## Materials and Methods

### Plasmid construction, siRNA and transfection

Plasmids used as templates containing the tandem FK506-binding protein domain (2xFKBP) and the mutant FRB domain (FRB\*) were previously constructed from components of the ARGENT Regulated Heterodimerization Kit provided by ARIAD (Fili et al., 2006). To generate the target fusion constructs, EGFP-2xFKBP was amplified by standard PCR using the GFP-Rab5a-target plasmid as template and the product subcloned into *AgeI*-*Bam*HI sites of pIRESpuro2 (Clontech). For EGFP-2xFKBP-paxillin, amplified paxillin was subcloned into the *NotI* site behind the tandem FKBP fragment.

To generate the recruitment fusion constructs, mRFP-FLAG-FRB\* was amplified using mRFP-FLAG-FRB plasmid as template and subcloned into *Hind*III-*Xho*I sites of pcDNA3.1(+)-hyg (Invitrogen). For mRFP-FLAG-FRB\*-MEK1EE, amplified MEK1EE was subcloned into the *Bam*HI-*Xho*I sites behind the FRB fragment. Site-directed mutagenesis of MEK1 (S218E and S222E) was performed by overlap extension. NRK cells were transfected with DNA by lipofection following the manufacturer's protocol (Roche).

siRNA was transfected at 25 nM with Lullaby (OZ Biosciences) according from recommendations of the manufacturer. siRNA against aPKC $\epsilon$  was obtained from Qiagen with following target sequence: 5'-GCAACUCUGGUUCAUAAdTdT-3'.

### Cell culture and wound assay

Normal rat kidney (NRK) cells were cultured in Dulbecco's modified Eagle medium and 10% fetal calf serum under 5% CO<sub>2</sub> on Falcon plastic dishes. Stable cell lines were selected with puromycin and hygromycin. Wounds were inflicted by scratching the surface with a plastic pipette tip. Time-lapse images of cell migration were recorded every 20 minutes using an inverted microscope (Zeiss Axiovert 135TV or Nikon Eclipse TE2000) equipped with a 10 $\times$ , 5.6 NA Plan-Neofluor air objective and a Hamamatsu Orca ER CCD or Andor Ixon single photon CCD camera at 37°C and 5% CO<sub>2</sub>. Quantification of the speed of wound closure and of individual cells was performed using Metamorph, Tracker and Mathematik.

### Immunofluorescence

Cells attached to coverslips, fixed in 4% paraformaldehyde and permeabilized with 0.1% Triton X-100 were incubated with the primary antibody for 45 minutes followed by incubated with the appropriate secondary antibody. Coverslips were mounted using Prolong (Molecular Probes/Invitrogen). ERK1/2-*P* antibody was obtained from Cell Signaling, secondary antibody coupled to Alexa Fluor 647 was from Molecular Probes. Images were acquired using a confocal laser scanning microscope (Zeiss AxioPlan 2) equipped with a 63 $\times$ , 1.4 NA Plan-Apochromat oil immersion objective at room temperature.

### Immunoprecipitation and immunodetection

For whole-cell extracts, cells were lysed directly on plates in Laemmli sample buffer. For immunoprecipitation, cells were lysed in 20 mM Tris-HCl (pH 7.4), 100 mM NaCl, 1 mM MgCl<sub>2</sub>, 0.1 mM dithiothreitol, 1% Triton X-100, EDTA and 10% glycerol. SDS-PAGE was performed using NuPAGE 4-12% Bis-Tris gels (Invitrogen). Proteins were transferred on Hybond membranes (GE) and visualized with a chemiluminescent detection system (ECL: Amersham). Primary antibodies were obtained from Santa Cruz (paxillin), Cell Signaling (ERK1/2-*P*) or Abcam (paxillin Ser126-*P*). The anti-GFP and anti-FLAG monoclonal antibodies were provided by Cancer Research UK, Research Services. For the detection of ERK1/2 and paxillin cells were scratched, allowed to migrate for different times, treated with inhibitors and rapalogue and then harvested in Laemmli sample buffer. Quantification of blots was performed with ImageJ software.

### TIRF live cell imaging and focal adhesion disassembly quantification

Stable NRK cell lines were grown in fibronectin-coated MatTek dishes to confluence. Cells were wounded to induce cell migration. Time-lapse images were acquired using an inverted microscope (Nikon TE2000) with a Apo TIRF 100 $\times$ , 1.49 NA oil objective and a CCD camera (Cascade-II, Photometrics) at 37°C. To quantify the rates of focal adhesion assembly and disassembly, the fluorescence intensity of individual adhesions was measured over time using Metamorph. Changes in fluorescence intensity were normalized to the maximal value and plotted in semilogarithmic plots as a function of time. The rates were determined from the slopes of these graphs [assembly:  $\ln(x/\text{minutes})$ , disassembly:  $\ln(\text{max}/\text{minutes})$ ].

### Quantification of the zyxin spots

Non confluent double stable NRK cells overexpressing GFP-FKBP-paxillin and RFP-FRB-MEK1EE were treated for 3 hours with G6983 (5  $\mu$ M) and/or rapalogue (300 nM). The control cells were treated with ethanol and DMSO. Cells were fixed in paraformaldehyde (4%) and permeabilized with Triton X-100 (1%), then stained for zyxin (Santa Cruz).

For the quantification of the paxillin spots, an Array Scan II and the Cellomics analysis program were employed. Each cell was identified by nuclear staining (DAPI) and actin staining (phalloidin). Each area of interest for the analysis (spot or fibre) was delimited and represented as an object. The number of paxillin spots as well as the total area of stress fibres per cell were measured (Rosse et al., 2009). The statistical analysis was performed with the software Prism\* using an ANOVA statistical test.

This work was supported by Cancer Research UK. C.R. was also supported by a fellowship from FEBS. We thank Natalie Fili and Banafshe Larijani for providing GFP-Rab5a-target and mRFP-FLAG-FRB\* plasmids. We thank all members of the Light Microscopy Laboratory for help and all members of the Protein Phosphorylation Lab for stimulating discussions.

Supplementary material available online at

<http://jcs.biologists.org/cgi/content/full/123/16/2725/DC1>

## References

Bhatt, A., Kaverina, I., Otey, C. and Huttenlocher, A. (2002). Regulation of focal complex composition and disassembly by the calcium-dependent protease calpain. *J. Cell Sci.* **115**, 3415-3425.

- Broussard, J. A., Webb, D. J. and Kaverina, I. (2008). Asymmetric focal adhesion disassembly in motile cells. *Curr. Opin. Cell Biol.* **20**, 85-90.
- Campbell, D. H., Sutherland, R. L. and Daly, R. J. (1999). Signaling pathways and structural domains required for phosphorylation of EMS1/cortactin. *Cancer Res.* **59**, 5376-5385.
- Carragher, N. O. and Frame, M. C. (2004). Focal adhesion and actin dynamics: a place where kinases and proteases meet to promote invasion. *Trends Cell Biol.* **14**, 241-249.
- Etienne-Manneville, S. and Hall, A. (2003). Cdc42 regulates GSK-3 $\beta$  and adenomatous polyposis coli to control cell polarity. *Nature* **421**, 753-756.
- Etienne-Manneville, S., Manneville, J. B., Nicholls, S., Ferenczi, M. A. and Hall, A. (2005). Cdc42 and Par6-PKC $\zeta$  regulate the spatially localized association of Dlg1 and APC to control cell polarization. *J. Cell Biol.* **170**, 895-901.
- Favata, M. F., Horiuchi, K. Y., Manos, E. J., Daulerio, A. J., Stradley, D. A., Feese, W. S., Van Dyk, D. E., Pitts, W. J., Earl, R. A., Hobbs, F. et al. (1998). Identification of a novel inhibitor of mitogen-activated protein kinase kinase. *J. Biol. Chem.* **273**, 18623-18632.
- Fili, N., Calleja, V., Woscholski, R., Parker, P. J. and Larijani, B. (2006). Compartmental signal modulation: Endosomal phosphatidylinositol 3-phosphate controls endosome morphology and selective cargo sorting. *Proc. Natl. Acad. Sci. USA* **103**, 15473-15478.
- Fincham, V. J., James, M., Frame, M. C. and Winder, S. J. (2000). Active ERK/MAP kinase is targeted to newly forming cell-matrix adhesions by integrin engagement and v-Src. *EMBO J.* **19**, 2911-2923.
- Franco, S. J., Rodgers, M. A., Perrin, B. J., Han, J., Bennin, D. A., Critchley, D. R. and Huttenlocher, A. (2004). Calpain-mediated proteolysis of talin regulates adhesion dynamics. *Nat. Cell Biol.* **6**, 977-983.
- Inoue, T., Heo, W. D., Grimley, J. S., Wandless, T. J. and Meyer, T. (2005). An inducible translocation strategy to rapidly activate and inhibit small GTPase signaling pathways. *Nat. Methods* **2**, 415-418.
- Ishibe, S., Joly, D., Zhu, X. and Cantley, L. G. (2003). Phosphorylation-dependent paxillin-ERK association mediates hepatocyte growth factor-stimulated epithelial morphogenesis. *Mol. Cell* **12**, 1275-1285.
- Kiely, P. A., Baillie, G. S., Barrett, R., Buckley, D. A., Adams, D. R., Houslay, M. D. and O'Connor, R. (2009). Phosphorylation of RACK1 on tyrosine 52 by c-Abl is required for IGF-I-mediated regulation of focal adhesion kinase (FAK). *J. Biol. Chem.* **284**, 20263-20274.
- Klemke, R. L., Cai, S., Giannini, A. L., Gallagher, P. J., de Lanerolle, P. and Cheresch, D. A. (1997). Regulation of cell motility by mitogen-activated protein kinase. *J. Cell Biol.* **137**, 481-492.
- Lai, F. P., Szczodrak, M., Oelkers, J. M., Ladwein, M., Acconcia, F., Benesch, S., Auinger, S., Faix, J., Small, J. V., Polo, S. et al. (2009). Cortactin promotes migration and PDGF-induced actin reorganization by signaling to Rho-GTPases. *Mol. Biol. Cell.* **20**, 3209-3223.
- Liu, Z. X., Yu, C. F., Nickel, C., Thomas, S. and Cantley, L. G. (2002). Hepatocyte growth factor induces ERK-dependent paxillin phosphorylation and regulates paxillin-focal adhesion kinase association. *J. Biol. Chem.* **277**, 10452-10458.
- Lock, J. G., Wehrle-Haller, B. and Stromblad, S. (2008). Cell-matrix adhesion complexes: master control machinery of cell migration. *Semin. Cancer Biol.* **18**, 65-76.
- Mansour, S. J., Matten, W. T., Hermann, A. S., Candia, J. M., Rong, S., Fukasawa, K., Vande Woude, G. F. and Ahn, N. G. (1994). Transformation of mammalian cells by constitutively active MAP kinase kinase. *Science* **265**, 966-970.
- Nguyen, D. H., Catling, A. D., Webb, D. J., Sankovic, M., Walker, L. A., Somlyo, A. V., Weber, M. J. and Gonias, S. L. (1999). Myosin light chain kinase functions downstream of Ras/ERK to promote migration of urokinase-type plasminogen activator-stimulated cells in an integrin-selective manner. *J. Cell Biol.* **146**, 149-164.
- Nishimura, T. and Kaibuchi, K. (2007). Numb controls integrin endocytosis for directional cell migration with aPKC and PAR-3. *Dev. Cell* **13**, 15-28.
- Pawlak, G. and Helfman, D. M. (2002). MEK mediates v-Src-induced disruption of the actin cytoskeleton via inactivation of the Rho-ROCK-LIM kinase pathway. *J. Biol. Chem.* **277**, 26927-26933.
- Ridley, A. J., Schwartz, M. A., Burridge, K., Firtel, R. A., Ginsberg, M. H., Borisy, G., Parsons, J. T. and Horwitz, A. R. (2003). Cell migration: integrating signals from front to back. *Science* **302**, 1704-1709.
- Rosse, C., Formstecher, E., Boeckeler, K., Zhao, Y., Kremerskothen, J., White, M., Camonis, J. and Parker, P. J. (2009). An aPKC-Exocyst complex controls Paxillin phosphorylation and migration through localised JNK1 activation. *PLoS Biol.* **7**, e1000235.
- Slack-Davis, J. K., Eblen, S. T., Zecevic, M., Boerner, S. A., Tarcsafalvi, A., Diaz, H. B., Marshall, M. S., Weber, M. J., Parsons, J. T. and Catling, A. D. (2003). PAK1 phosphorylation of MEK1 regulates fibronectin-stimulated MAPK activation. *J. Cell Biol.* **162**, 281-291.
- Sun, R., Gao, P., Chen, L., Ma, D., Wang, J., Oppenheim, J. J. and Zhang, N. (2005). Protein kinase C  $\zeta$  is required for epidermal growth factor-induced chemotaxis of human breast cancer cells. *Cancer Res.* **65**, 1433-1441.
- Suzuki, A. and Ohno, S. (2006). The PAR-aPKC system: lessons in polarity. *J. Cell Sci.* **119**, 979-987.
- Varnai, P., Thyagarajan, B., Rohacs, T. and Balla, T. (2006). Rapidly inducible changes in phosphatidylinositol 4,5-bisphosphate levels influence multiple regulatory functions of the lipid in intact living cells. *J. Cell Biol.* **175**, 377-382.
- Webb, D. J., Donais, K., Whitmore, L. A., Thomas, S. M., Turner, C. E., Parsons, J. T. and Horwitz, A. F. (2004). FAK-Src signalling through paxillin, ERK and MLCK regulates adhesion disassembly. *Nat. Cell Biol.* **6**, 154-161.
- Webb, D. J., Schroeder, M. J., Brame, C. J., Whitmore, L., Shabanowitz, J., Hunt, D. F. and Horwitz, A. R. (2005). Paxillin phosphorylation sites mapped by mass spectrometry. *J. Cell Sci.* **118**, 4925-4929.
- Woodrow, M. A., Woods, D., Cherwinski, H. M., Stokoe, D. and McMahon, M. (2003). Ras-induced serine phosphorylation of the focal adhesion protein paxillin is mediated by the Raf->MEK->ERK pathway. *Exp. Cell Res.* **287**, 325-338.
- Xu, L. and Deng, X. (2006). Protein kinase Ciota promotes nicotine-induced migration and invasion of cancer cells via phosphorylation of micro- and m-calpains. *J. Biol. Chem.* **281**, 4457-4466.
- Yeaman, C., Grindstaff, K. K., Wright, J. R. and Nelson, W. J. (2001). Sec6/8 complexes on trans-Golgi network and plasma membrane regulate late stages of exocytosis in mammalian cells. *J. Cell Biol.* **155**, 593-604.
- Zaidel-Bar, R., Ballestrem, C., Kam, Z. and Geiger, B. (2003). Early molecular events in the assembly of matrix adhesions at the leading edge of migrating cells. *J. Cell Sci.* **116**, 4605-4613.